

# NJC

Accepted Manuscript



This is an *Accepted Manuscript*, which has been through the Royal Society of Chemistry peer review process and has been accepted for publication.

*Accepted Manuscripts* are published online shortly after acceptance, before technical editing, formatting and proof reading. Using this free service, authors can make their results available to the community, in citable form, before we publish the edited article. We will replace this *Accepted Manuscript* with the edited and formatted *Advance Article* as soon as it is available.

You can find more information about *Accepted Manuscripts* in the [Information for Authors](#).

Please note that technical editing may introduce minor changes to the text and/or graphics, which may alter content. The journal's standard [Terms & Conditions](#) and the [Ethical guidelines](#) still apply. In no event shall the Royal Society of Chemistry be held responsible for any errors or omissions in this *Accepted Manuscript* or any consequences arising from the use of any information it contains.

## A novel white-light-emitting conjugated polymer derived from polyfluorene with hyperbranched structure

Jing Sun,<sup>ab</sup> Junli Yang,<sup>ab</sup> Chongyang Zhang,<sup>c</sup> Hua Wang,<sup>ab</sup> Jie Li,<sup>ab</sup> Shijian Su,<sup>c</sup> Huixia Xu,<sup>ab</sup> Tiaomei Zhang,<sup>ab</sup> Yuling Wu,<sup>ab</sup> Wai-Yeung Wong<sup>d</sup> and Bingshe Xu<sup>\*ab</sup>

**Abstract:** A series of novel hyperbranched conjugated polymers containing the red phosphorescent iridium complexes to realize the white-light emission have been designed and synthesized. The iridium complexes, tris[1-phenylisoquinolino-C2,N]iridium (III) ( $\text{Ir}(\text{piq})_3$ ) as red emitter, are covalently connected with the polyfluorene segments as blue emitter. Based on the hyperbranched structure, the conjugated polymers with large steric hindrance can effectively suppress the triplet-triplet annihilation. Simultaneously, the synthesized polymers express relatively thermostability, photophysical properties with a higher fluorescence quantum yield (57 %~77 %) and electrochemistry properties. By incorporating about 0.1 mol% of  $\text{Ir}(\text{piq})_3$  into the conjugated polymers, the white-light emission could be achieved. Single-active-layer polymer light emitting devices with the configuration of ITO / PEDOT: PSS / polymer / TPBI / LiF / Al have been fabricated. Among all devices, the device of PF- $\text{Ir}(\text{piq})_3$ 100 exhibits Commission Internationale de l'Eclairage coordinate of (0.30, 0.23), which close to that of pure white light. It indicates that the hyperbranched polymers mixed the fluorescence and phosphorescence emission would be the promising white-light materials.

<sup>a</sup> Key Laboratory of Interface Science and Engineering in Advanced Materials, Taiyuan University of Technology, Ministry of Education, No. 79, West Yingze Street, Taiyuan 030024, P. R. China. E-mail: xubs@tyut.edu.cn (B.S. Xu)

<sup>b</sup> Research Center of Advanced Materials Science and Technology, Taiyuan University of Technology, No. 79, West Yingze Street, Taiyuan 030024, P. R. China.

<sup>c</sup> Institute of Molecular Functional Materials, Department of Chemistry, Institute of Advanced Materials, Hong Kong Baptist University, Hong Kong, P. R. China.

<sup>d</sup> State Key Laboratory of Luminescent Materials and Devices and Institute of Polymer Optoelectronic Materials and Devices, South China University of Technology, Guangzhou 510640, P. R. China.

**Key words:** Hyperbranched, Synthesis, Luminescence, Photophysics

## 1. Introduction

In the last decades, white polymer light emitting devices (WPLEDs) have received great attention due to continuous advance toward their favorable properties such as homogenous large-area emission, good color rendering, and potential realization on flexible substrates.<sup>1-3</sup> WPLEDs could usually be fabricated by doping of the orange fluorescent or phosphorescent dyes with narrow energy band in a blue-emitting polymer host or blending heterochromatic polymers,<sup>4-5</sup> respectively. While these blended systems induce problems of phase separation between different components in PLEDs, which seriously damage the interfaces and reduce device performance of WPLEDs.<sup>6-10</sup> Hence, it is necessary to design and prepare single white-light-emitting polymers<sup>11-17</sup> introduced different emitting units by covalent bond and used as active single-layer for reducing heterogeneous interfaces and improving device performance of WPLEDs. This approach has been demonstrated in several white-light-emitting polymers such as polyfluorene incorporated fluorescent or phosphorescent emitting units that obtains better achievements. Moon et al.<sup>13</sup> have synthesized linear white-light polymers incorporated orange quinoxaline derivative to the polyfluorene host which exhibits good white-light emission. Wang et al.<sup>18-22</sup> have developed several series of single white-emitting polymers with fluorescent triphenylamine derivatives as orange emitter that show perfect electroluminescent performance. Cao et al.<sup>23-28</sup> have also studied a series of fluorescence/phosphorescence hybrid single white-emitting polymers with modified polyfluorene segments to give blue emission, and iridium complexes attached to the polyfluorene backbone on the main chain or side chain to give red phosphorescent emission. The electroluminescent efficiency of the resulting WPLEDs has also been greatly improved. However, the intermolecular interaction can't be significantly suppressed in the linear phosphorescent polymers.<sup>31</sup>

Recently, hyperbranched polymers<sup>29-32</sup> have been proposed as an alternative approach to embed different emitters in polymeric systems due to facile tunable properties through modification of the cores, branches or surface groups. At the same time, it also possesses a three-dimensional structure with high solubility, minimization of unfavorable crystallization and excellent film formability. The

most-important factor is that the highly branched and globular features can significantly suppress both intermolecular interactions and aggregation between the adjacent iridium complexes. Cao et al.<sup>29</sup> have reported a red phosphorescent hyperbranched polymer utilized the red phosphorescent iridium complexes as the cores with excellent electroluminescent properties which exhibits potential of the hyperbranched polymers in the white-light emission.

In this paper, a novel series of hyperbranched white-light polymers utilized the polyfluorene as the blue emission branches and Ir(piq)<sub>3</sub> as the red emission cores<sup>33-36</sup> have been designed and synthesized. Herein, the photophysical properties of solution- and film-states were described and investigated in details. By tuning the mole ratios of Ir(piq)<sub>3</sub>, the white emission from two individual emission species in a single polymer has been achieved. It is found that the hyperbranched polymers have more efficient energy transfer<sup>37-40</sup> from the polyfluorene segments to Ir(piq)<sub>3</sub> units, which could be a candidate of the high-efficiency single white-light polymers.

## 2. Experimental Section

### 2.1 Materials

Commercially available reagents were used without further purification, unless stated otherwise. The solvents (e.g. THF, CHCl<sub>3</sub> and toluene) were purified by routine procedures and distilled under dry nitrogen before using. All manipulations involving air-sensitive reagents were performed under dry nitrogen protection.

### 2.2 Instruments and characterization

<sup>1</sup>H NMR spectra were recorded on a Bruker DRX 600 spectrometer, at 600 MHz in deuterated chloroform with tetramethylsilane as a reference at room temperature. Elemental analyses were performed on a Vario EL elemental analyzer and TOF-MS was recorded on Bruker MALDI-TOF. The molecular weights of the polymers were determined by waters GPC 2410 using THF as the eluent. Thermogravimetric (TG) analyses were performed on a Netzsch TG 209 F3 at a heating rate of 10 °C min<sup>-1</sup>. The differential scan calorimetry (DSC) curves were measured on a Netzsch DSC 204 under nitrogen flow at a heating rate of 5 °C min<sup>-1</sup>. UV-Vis absorption spectra were recorded on a Hitachi U-3900 spectrophotometer in the CHCl<sub>3</sub> solution of 5×10<sup>-6</sup> mol L<sup>-1</sup> or in the thin solid films.

The PL spectra were recorded on a Fluoromax-4 spectrophotometer in  $10^{-6}$  mol L<sup>-1</sup> CHCl<sub>3</sub> solution or in the thin solid films excited at 365 nm. The PL quantum efficiencies ( $\Phi_{\text{PL}}$ ) were measured using the integrating sphere in diluted CHCl<sub>3</sub> solution and films excited at 365 nm, respectively. Cyclic voltammetry (CV) data were measured on the Autolab/PG STAT302 electrochemical workstation using tetrabutylammonium perchlorate (0.1 mol L<sup>-1</sup>) in acetonitrile as the electrolyte at a scan rate of 50 mV s<sup>-1</sup> at room temperature under nitrogen atmosphere. A conventional three-electrode configuration was used to measure with two platinum plates as the working electrode and counter electrode, and calomel electrode as the reference electrode at room temperature.

### 2.3 Synthesis and characterization

#### 2.3.1 1-(4-bromophenyl)-isoquinoline (L)

The 1-chloroisoquinoline (1.63 g, 10 mmol), 4-bromophenylboronic acid (2.00 g, 10 mmol) and tetrakis(triphenylphosphine)palladium (Pd(PPh<sub>3</sub>)<sub>4</sub>) (34.68 mg, 0.03 mmol) were dissolved in the mixed solution of degassed toluene (20 mL) and ethanol (5 mL). Then an aqueous solution of 2 mol L<sup>-1</sup> Na<sub>2</sub>CO<sub>3</sub> (8 mL) was added to the stirred mixture. Subsequently, the resulting mixture was slowly heated to 94 °C and stirred for overnight. After cooling to room temperature, the reaction mixture was washed with water, dried under anhydrous magnesium sulfate. Finally, the solvent was removed and the residue was purified by column chromatography (silica gel, dichloromethane/hexane=1:4). A white needle crystal was isolated (yield: 2.21 g, 78 %). m. p. 80–85 °C. <sup>1</sup>H NMR: (600 MHz, CDCl<sub>3</sub>):  $\delta$ (ppm)= 8.61 (d, J=5.4 Hz, 1 H), 7.98 (d, J=3 Hz, 2 H), 7.74–7.53 (m, 7 H). <sup>13</sup>C NMR: (600MHz, CDCl<sub>3</sub>):  $\delta$ (ppm)= 159.6, 142.4, 138.7, 137.0, 131.7, 130.3, 127.5, 127.3, 126.7, 123.2, 120.3. Element Anal. Calcd (%): C, 63.40; H, 3.55; N, 4.93. Found (%): C, 63.47; H, 3.75; N, 4.86.

#### 2.3.2 Tri(2-(4-bromophenyl)-isoquinoline) iridium (III) (Ir(piqBr)<sub>3</sub>) (M1)

Tri(acetylacetonato)iridium (III) (244 mg, 0.5 mmol), 1-(4-bromophenyl)-isoquinoline (497 mg, 1.75 mmol) were added into the anhydrous glycerol (15 mL). The reaction solution was slowly heated to 220 °C and stirred for 24 h. After cooling, more water was added, and then a red precipitate was collected, washed by water, filtered and dried in turn. Finally, the precipitate was purified by column chromatography (silica gel, dichloromethane/petroleum ether=1:8) to get red powder (yield: 104 mg, 20 %). m. p. >320 °C. <sup>1</sup>H NMR: (600 MHz, CDCl<sub>3</sub>):  $\delta$ (ppm)= 8.87 (dd, J<sub>1</sub>=7.2 Hz,

$J_2=3$  Hz, 3 H), 8.03 (d,  $J=8.4$  Hz, 3 H), 7.76 (dd,  $J_1=5.4$  Hz,  $J_2=3$  Hz, 3 H), 7.70–7.67 (m, 6 H), 7.29 (d,  $J=6.6$  Hz, 2 H), 7.15 (d,  $J=6.6$  Hz, 3 H), 7.13 (dd,  $J_1=8.4$  Hz,  $J_2=2.4$  Hz, 3 H), 7.03 (d,  $J=1.8$  Hz, 3 H).  $^{13}\text{C}$  NMR: (600 MHz,  $\text{CDCl}_3$ ):  $\delta(\text{ppm})= 166.9, 165.6, 144.2, 139.7, 139.3, 136.9, 131.5, 131.0, 130.7, 129.0, 128.1, 127.5, 127.3, 123.4, 120.1$ . Element Anal. Calcd (%): C, 51.89; H, 2.61; N, 4.03. Found (%): C, 52.01; H, 2.69; N, 3.92. TOF-MS, measured, 1039.07, calcd, 1041.64.

### 2.3.3 Polymerization

Hyperbranched polymers of PF-Ir(piq)<sub>3</sub>m (m= 25, 50, 100 and 500) were synthesized by Suzuki crossing reaction. Reaction monomers 2,7-Bis(4,4,5,5-tetramethyl-1,3,2-dioxaborolan-2-yl)-9,9-dioctylfluorene (M2), 9,9-dioctylfluorene-2,7-dibromofluorene (M3) and Ir(piqBr)<sub>3</sub> (M1) were synthesized according to reference.<sup>41-42</sup> The monomers of M1, M2, and M3 were dissolved in degassed toluene (20 mL), and then stirred under nitrogen atmosphere. Then Pd(PPh<sub>3</sub>)<sub>4</sub> (2 mol%) was added to the reaction solution and stirred for about 30 min. The methyl trioctyl ammonium chloride (Aliquat 336°) and aqueous solution of 2 M K<sub>2</sub>CO<sub>3</sub> (10 mL) were added, and the mixture was stirred and slowly heated to the refluxed temperature for 48 h. Subsequently, the polymer was capped by adding benzenboronic acid (20 mg) with continuous stirred for 12 h, and then bromobenzene (0.2 mL) was added with continuously reaction for another 12 h. Finally, the whole reaction solution was poured into the stirred methanol. The precipitated polymer was collected by filtration and purified with acetone in soxhlet extraction to remove the small molecules and catalyst residue. The crude product was purified by column chromatography (silica gel, dichloromethane: THF=10: 1) to get the solid powder.

**2.3.3.1. PF-Ir(piq)<sub>3</sub>500.** M2 (642.6 mg, 1 mmol), M3 (540.2 mg, 0.985 mmol), and M1 (10.42 mg, 0.01 mmol) were added in the polymerization. The product was pink-white powder (yield: 414 mg, 53 %).  $^1\text{H}$  NMR: (600 MHz,  $\text{CDCl}_3$ ):  $\delta(\text{ppm})= 7.88$  (1 H, Ar–H), 7.67–7.66 (2 H, Ar–H), 2.15 (2 H, CH<sub>2</sub>), 1.28–1.02 (10 H, 5 CH<sub>2</sub>), 0.89–0.81 (5 H, CH<sub>2</sub>, CH<sub>3</sub>). Element Anal. Calcd (%): C, 89.46; H, 10.24. Found (%): C, 89.17; H, 9.79.

**2.3.3.2. PF-Ir(piq)<sub>3</sub>100.** M2 (642.6 mg, 1 mmol), M3 (546.8 mg, 0.997 mmol), and M1 (2.08 mg, 0.002 mmol) were added in the polymerization. The product was light-yellow powder (yield: 371 mg, 47.6 %).  $^1\text{H}$  NMR: (600 MHz,  $\text{CDCl}_3$ ):  $\delta(\text{ppm})= 7.84$  (1H, Ar–H), 7.74–7.63 (2 H, Ar–H), 2.13

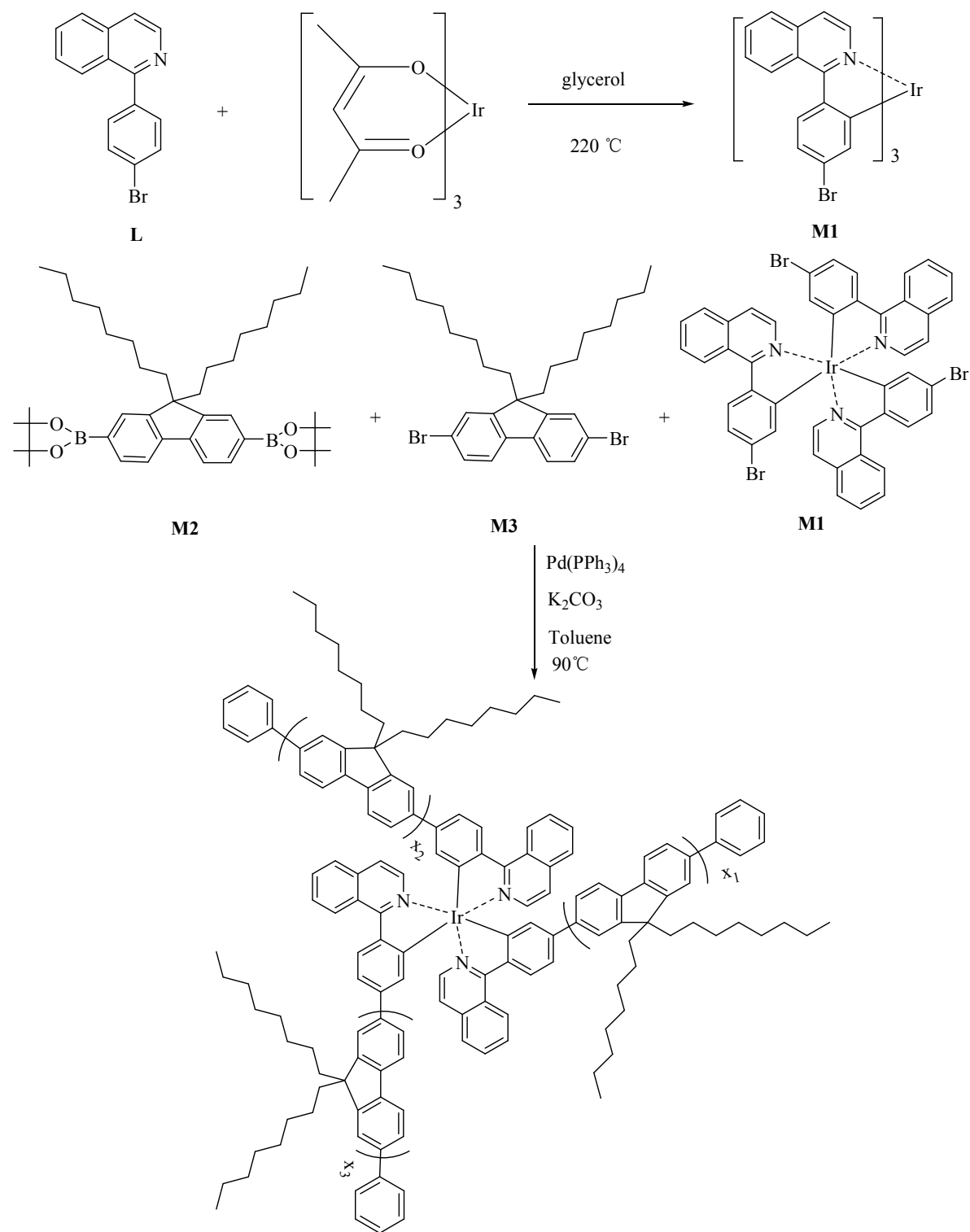
(2 H, CH<sub>2</sub>), 1.24–1.05 (10 H, 5 CH<sub>2</sub>), 0.86–0.74 (5 H, CH<sub>2</sub>, CH<sub>3</sub>). Element Anal. Calcd (%): C, 89.61; H, 10.29. Found (%): C, 89.58; H, 9.52.

**2.3.3.3. PF-Ir(piq)<sub>3</sub>50.** M2 (642.6 mg, 1 mmol), M3 (547.6 mg, 0.9985 mmol), and M1 (1.04 mg, 0.001 mmol) were added in the polymerization. The product was light-yellow powder (yield: 475 mg, 61 %). <sup>1</sup>H NMR: (600 MHz, CDCl<sub>3</sub>): δ(ppm)= 7.84 (1 H, Ar–H), 7.74–7.63 (2 H, Ar–H), 2.13 (2 H, CH<sub>2</sub>), 1.24–1.05 (10 H, 5 CH<sub>2</sub>), 0.86–0.74 (5 H, CH<sub>2</sub>, CH<sub>3</sub>). Element Anal. Calcd (%): C, 89.67; H, 10.30. Found (%): C, 89.40; H, 10.09.

**2.3.3.4. PF-Ir(piq)<sub>3</sub>25.** M2 (642.6 mg, 1 mmol), M3 (548.0 mg, 0.9993 mmol), and M1 (0.52 mg, 0.0005 mmol) were added in the polymerization. The product was white-gray powder (yield: 466 mg, 59 %). <sup>1</sup>H NMR: (600 MHz, CDCl<sub>3</sub>): δ(ppm)= 7.84 (1 H, Ar–H), 7.73–7.64 (2 H, Ar–H), 2.12 (2 H, CH<sub>2</sub>), 1.25–1.02 (10 H, 5 CH<sub>2</sub>), 0.90–0.73 (5 H, CH<sub>2</sub>, CH<sub>3</sub>). Element Anal. Calcd (%): C, 89.68; H, 10.31. Found (%): C, 89.14; H, 10.01.

## 2.4 Device fabrication

The fabrication process of the WPLEDs followed as standard procedure described below. Each glass substrate coated with transparent indium-tin oxide (ITO) was cleaned with detergent, deionized water and acetone sequentially. Then, the substrates were dried on a plate and treated with oxygen plasma. Poly(3,4-enthylene-dioxythiophene):poly(styrene-sulfonate) (PEDOT: PSS, Clevios P VP AI 4083) as a hole-injection layer was coated onto the ITO substrate, and then annealed at 120 °C for 20 min under nitrogen atmosphere. Then, the light-emitting layer polymers of PF-Ir(piq)<sub>3</sub>m (m=25, 50, 100 and 500) dissolved in degassed toluene (10 mg mL<sup>-1</sup>) was coated onto the PEDOT:PSS film and annealed at 100 °C for 20 min. The multilayers of TPBI (40 nm) / LiF (1 nm) / Al (100 nm) were subsequently vacuum-evaporated onto the top of the active polymer layer (a defined active area of 0.12 cm<sup>2</sup>) under vacuum degree of 1×10<sup>-4</sup> Pa. The current density (J) -voltage (V) -luminance (L) characteristics of WPLEDs were recorded on Keithley 2400 source meter and L-2188 spot brightness meter. The Electroluminescent spectra were collected by using the SpectraScan PR655. All measurements were carried on at room temperature.



**Scheme 1** Synthetic route of the hyperbranched polymers PF-Ir(piq)<sub>3</sub>m (25, 50, 100 and 500).

### 3. Result and Discussion

#### 3.1 Synthesis and characterization of the hyperbranched polymers

The synthetic routes for Ir(piqBr)<sub>3</sub> and PF-Ir(piq)<sub>3</sub>m are depicted in Scheme 1. The 1-(4-bromophenyl)-isoquinoline was synthesized to prepare homoleptic iridium (III) complex via a Suzuki coupling reaction by the 1-chloroisoquinoline and 4-bromophenylboronic acid in a high yield. The hyperbranched polymers of PF-Ir(piq)<sub>3</sub>m were prepared by simple one-pot Suzuki polycondensation with a better yield, used the monomers of M1, M2 and M3, by tuning the feed ratios of 100:98.5:1 (m=500), 500:498.5:1 (m=100), 1000:998.5:1 (m=50) and 2000:1998.5:1 (m=25). The structures of the obtained polymer powder were confirmed by <sup>1</sup>H NMR. Due to the low content of Ir(piq)<sub>3</sub>, the proton peaks were dominated by the proton peaks from polyfluorene. In addition, the content of Ir(piq)<sub>3</sub> can't been measured by elemental analysis. In our work, all PF-Ir(piq)<sub>3</sub>m were readily soluble in common organic solvents, such as chloroform, toluene and THF. The number average molecular weights of the four hyperbranched polymers ranged from 9.2 to 18.9 kg mol<sup>-1</sup> are shown in Table 1. The polydispersity indices (PDI) show a broad distribution (1.96–4.38).

### 3.2 Thermal Analysis

The thermal properties of PF-Ir(piq)<sub>3</sub>m were determined by DSC and TG measurements. As shown in Fig. 1 and Table 1, the decomposition temperatures (T<sub>d</sub>) corresponding to 5 wt% weight loss of PF-Ir(piq)<sub>3</sub>m were all above 400 °C, which indicated their high thermal stability. Moreover, it also can be seen from DSC curves that all hyperbranched polymers exhibited rather higher glass transition temperatures (T<sub>g</sub>) above 130 °C compared with that of linear polymers ever reported,<sup>43-45</sup> which is since that the three-dimensional structure of hyperbranched polymers has large steric hindrance and the intermolecular crosslinking are enhanced by the branches. It is interesting that the T<sub>g</sub> of PF-Ir(piq)<sub>3</sub>m rose from 133 °C to 155 °C with increasing the mole ratio of Ir(piq)<sub>3</sub> in polymers from 0.025 mol% to 0.1 mol%, which would improve the device lifetime of the WPLEDs. However, the T<sub>g</sub> dropped to 139 °C when the mole ratio of Ir(piq)<sub>3</sub> in polymers increased to 0.5 mol%. At the high content of Ir(piq)<sub>3</sub>, the PF segments were interrupted by the red Ir complexes, and then the crosslinking between the adjacent molecules weakened that reduced the T<sub>g</sub>.

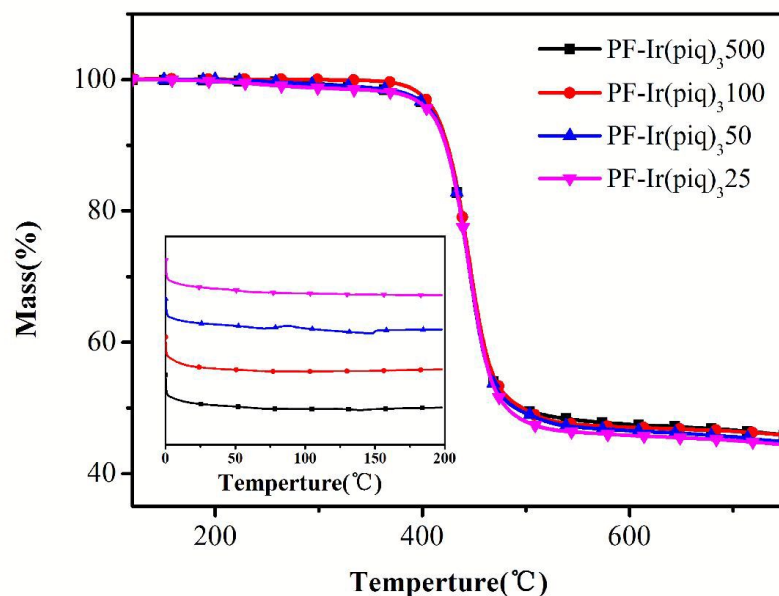


**Fig. 1** The TG and DSC curves of PF-Ir(piq)<sub>3</sub>m (25, 50, 100 and 500).

**Table 1** Molecular weight, thermal properties of PF-Ir(piq)<sub>3</sub>m (25, 50, 100 and 500).

Polymer	$M_n(\times 10^3)$	$M_w(\times 10^3)$	PDI	Ir(piq) <sub>3</sub> Feed ratio(mol%)	$T_d(^{\circ}\text{C})$	$T_g(^{\circ}\text{C})$
PF-Ir(piq) <sub>3</sub> 500	18.9	50.0	2.65	0.5	409	139
PF-Ir(piq) <sub>3</sub> 100	9.3	40.8	4.38	0.1	412	155
PF-Ir(piq) <sub>3</sub> 50	11.1	23.0	2.06	0.05	409	148
PF-Ir(piq) <sub>3</sub> 25	11.0	21.7	1.96	0.025	408	133

### 3.3 Electrochemical properties

The electrochemical properties of PF-Ir(piq)<sub>m</sub> are shown in Fig. 2. The HOMO levels of PF-Ir(piq)<sub>3</sub>m were calculated according to the empirical formulas  $E_{\text{HOMO}} = -(E_{\text{ox}} + 4.4)$  (eV).<sup>46</sup> The optical band gap was obtained from  $E_g = 1240/\lambda_{\text{edge}}$ , where the edge is the onset value of the absorption spectrum in films in the long-wavelength direction. From the HOMO levels and the optical gaps, the LUMO levels of PF-Ir(piq)<sub>3</sub>m could be determined. The HOMO level of PF-Ir(piq)<sub>3</sub>500 is at -5.76 eV, and the LUMO level is at -2.86 eV. Due to the low content of Ir(piq)<sub>3</sub>, this series of PF-Ir(piq)<sub>3</sub>m have similar HOMO and LUMO levels.

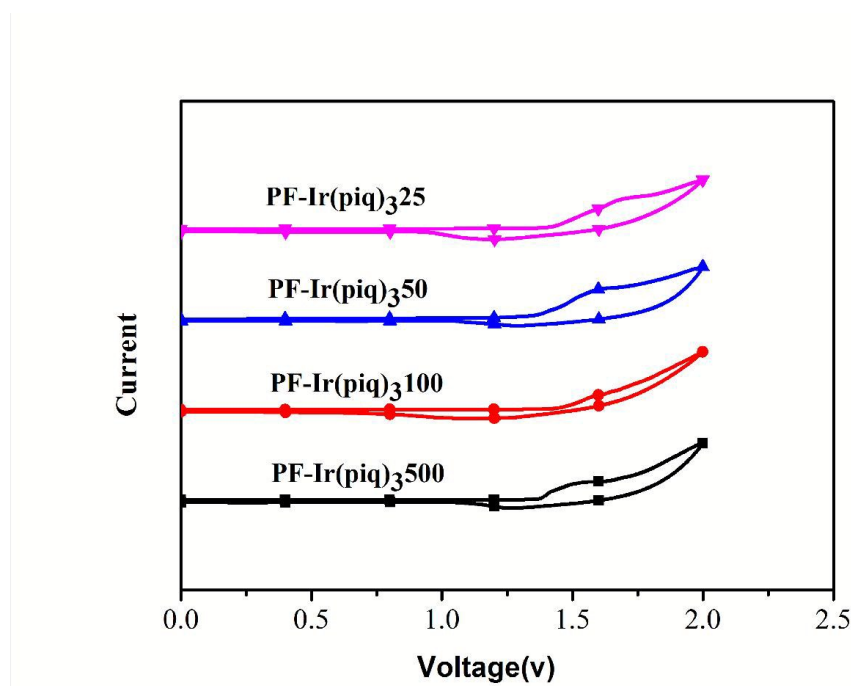


**Fig. 2** Cyclic voltammetry curves of PF-Ir(piq)<sub>3</sub>m (25, 50, 100 and 500).

### 3.4 Photophysical properties

In order to realize the efficient energy transfer from the blue polyfluorene (PF) segments to the red phosphors in the hyperbranched polymers, the absorption spectrum of Ir(piq)<sub>3</sub> and the PL spectra of PFO should overlap each other as shown in Fig. 3. We can see that the Ir(piq)<sub>3</sub> has a broad absorption band in the range of 380–570 nm, and the PL spectrum of the PFO is in the range of 400–570 nm, which express overlapped band in the range of 400–570 nm. It indicates that the possible Förster energy transfer from PF segments to Ir(piq)<sub>3</sub> phosphor, inducing in white light emission by combination of blue-light originated from PF segments and red-light originated from Ir(piq)<sub>3</sub> units.

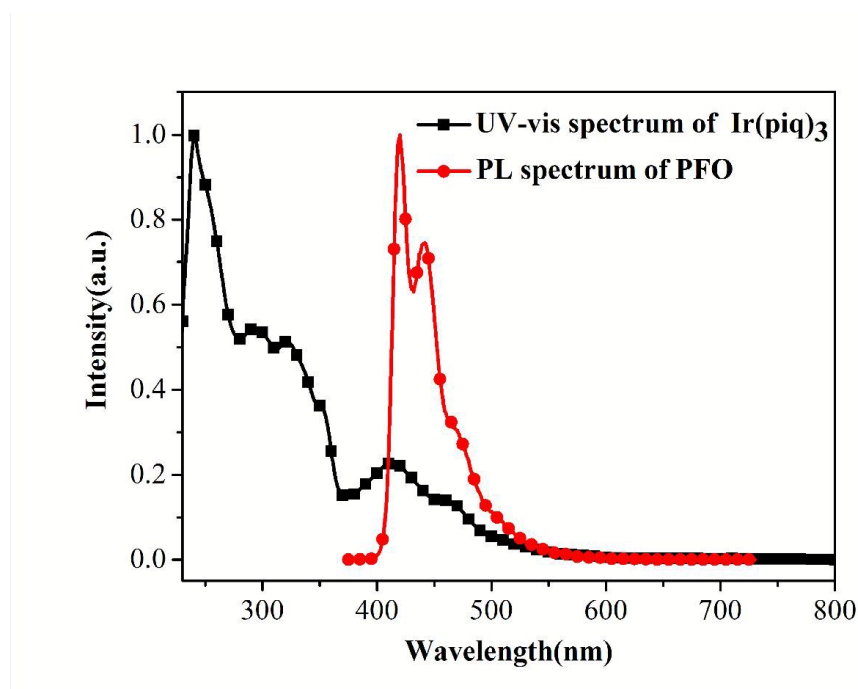


**Fig. 3** The UV-vis spectrum of Ir(piq)<sub>3</sub> in the diluted CHCl<sub>3</sub> solution and the PL spectrum of PFO in the diluted CHCl<sub>3</sub> solution.

As shown in Fig. 4 (a), the UV-vis spectra of the PF-Ir(piq)<sub>3</sub>m in the diluted CHCl<sub>3</sub> solution ( $5 \times 10^{-6}$  mol L<sup>-1</sup>) are dominated by a single peak with an absorption maximum ( $\lambda_{\text{abs}}$ ) around 384 nm, attributing to the  $\pi-\pi^*$  transition of the PF backbone. However, no distinct absorption peak corresponding to the Ir(piq)<sub>3</sub> is found due to the comparatively low content in PF-Ir(piq)<sub>3</sub>m. The PL spectra of PF-Ir(piq)<sub>3</sub>m in the diluted solution ( $10^{-6}$  mol L<sup>-1</sup>) are shown in Fig. 4 (b). There are three main emission peaks corresponding to blue emission of PF backbones, which locates at around 418 nm, 441 nm and 470 nm, respectively. Due to the low content of Ir(piq)<sub>3</sub>, the red emission can't be detected in all PL spectra of PF-Ir(piq)<sub>3</sub>m in the diluted solution. Above phenomena were almost identical with those former reported.<sup>37</sup> In addition, the  $\Phi_{\text{PL}}$  of PF-Ir(piq)<sub>3</sub> were measured in diluted CHCl<sub>3</sub> solution. As shown in table 1, the  $\Phi_{\text{PL}}$  in solutions increase along with the decreasing content of the Ir(piq)<sub>3</sub> units in PF-Ir(piq)<sub>3</sub>m because PF segments dominated in these hyperbranched polymers have high quantum efficiency. However, the increasing content of Ir(piq)<sub>3</sub> enhances the intersystem crossing, and simultaneously improves the energy transfer process from the singlet-emission polyfluorene to the triplet-emission Ir(piq)<sub>3</sub> that result in the energy loss in the transition from the singlet emission to the triplet emission.

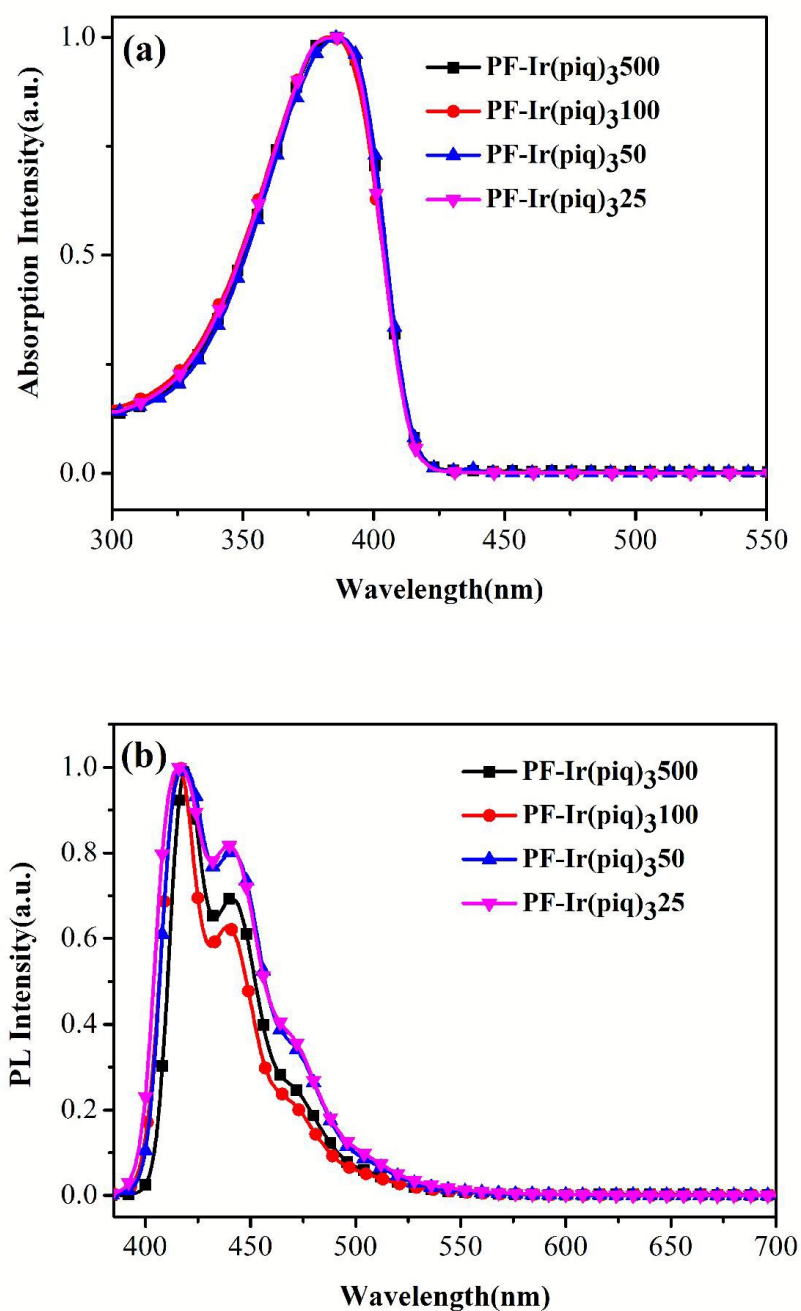


**Fig. 4** The UV-vis (a) and PL (b) spectra of PF-Ir(piq)<sub>3</sub>m (25, 50, 100 and 500) in the diluted CHCl<sub>3</sub> solution.

**Table 2** Photophysical and electrochemical properties of PF-Ir(piq)<sub>3</sub>m (25, 50, 100 and 500).

polymers	In solution/nm		In film/nm		$\Phi_{\text{PL}}$ (%)		HOMO (eV)	LUMO (eV)	$E_g$ (eV)
	$\lambda_{\text{abs}}$	$\lambda_{\text{PL}}$	$\lambda_{\text{abs}}$	$\lambda_{\text{PL}}$	solution	film			
PF-Ir(piq) <sub>3</sub> 500	385	417/441/469	380	420/444/471/626	57	5.8	-5.76	-2.86	2.90
PF-Ir(piq) <sub>3</sub> 100	383	415/441/469	378	422/446/475/625	60	10.0	-5.82	-2.90	2.92
PF-Ir(piq) <sub>3</sub> 50	385	417/441/470	380	420/444/476/626	71	14.5	-5.75	-2.84	2.91
PF-Ir(piq) <sub>3</sub> 25	384	415/439/469	378	420/444/473/625	77	7.3	-5.79	-2.87	2.92

Furthermore, the photophysical properties of the PF-Ir(piq)<sub>3</sub>m films coated on quartz substrates were also investigated. The Fig. 5(b) shows PL spectra of PF-Ir(piq)<sub>3</sub>m films. The PL spectra of the films are dominated by three blue main peaks located at about 421, 443 and 475 nm, and a red peak at around 625 nm with little shift compared to the solution. Because the hyperbranched structure has effectively enhanced the molecular rigidity by adding a PF branch. Different from diluted solution, the PL spectra of films exhibit obvious red emission peaks at around 625 nm, which are attributed to the high aggregation inducing more effective energy transfer between the inter- and intra-molecular interaction. Meanwhile, the red emission peaks of PF-Ir(piq)<sub>3</sub>m films show only about 6 nm bathochromic shift relative to that of Ir(piq)<sub>3</sub> (620 nm),<sup>34</sup> which is mainly since that the extended molecular chains of Ir(piq)<sub>3</sub> enhance the conjugacy in the PF-Ir(piq)<sub>3</sub>m and bring plenty of delocalized  $\pi$ -electrons around Ir(piq)<sub>3</sub>. At the same time, the hyperbranched structure with large steric hindrance could effectively suppress the PF chains aggregation and the red-shift of blue emission peak corresponding to PF, which is distinguished with white polymer based on PF with linear structure.<sup>24,25</sup> The strong blue emission indicates that the energy transfer from the host PF chains to the guest Ir(piq)<sub>3</sub> is incomplete. As shown in Table 2, it can be seen that the  $\Phi_{\text{PL}}$  of all PF-Ir(piq)<sub>3</sub>m films are much lower than those of diluted solution, which are similar to other white polymers.<sup>45</sup> This phenomenon could be rationalized by the high aggregation states inducing strong interaction between the adjacent molecules due to the intersystem crossing. The  $\Phi_{\text{PL}}$  in diluted solution decreases with the increasing content of Ir(piq)<sub>3</sub>, because the intersystem crossing between the PF segments and Ir(piq)<sub>3</sub> enhance that could reduce the radiative transition and the energy is consumed by non-radiative transition.

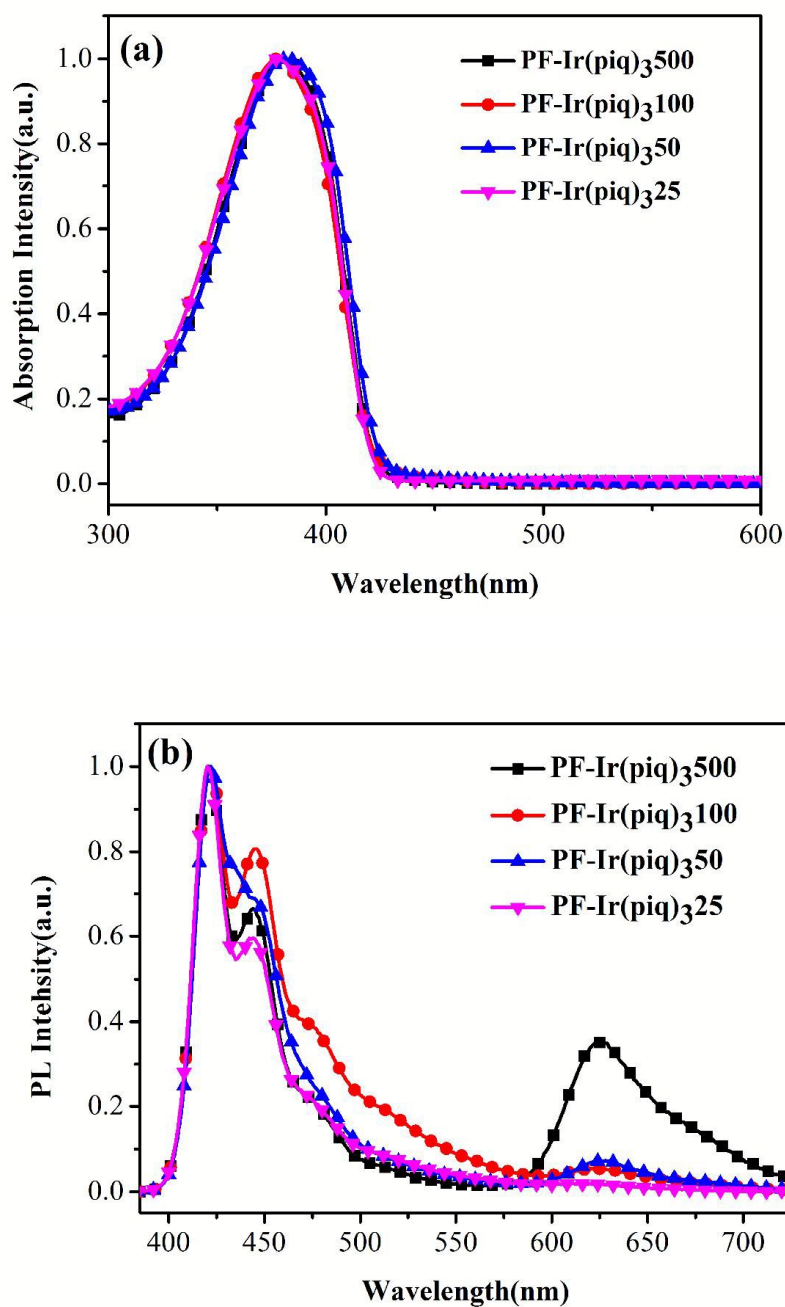


**Fig. 5** The UV-vis (a) and PL (b) spectra of the PF-Ir(piq)<sub>3</sub>m films.

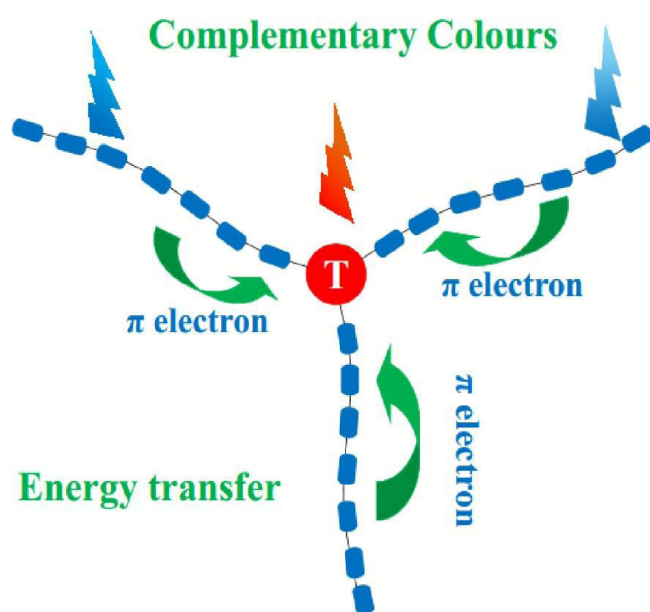


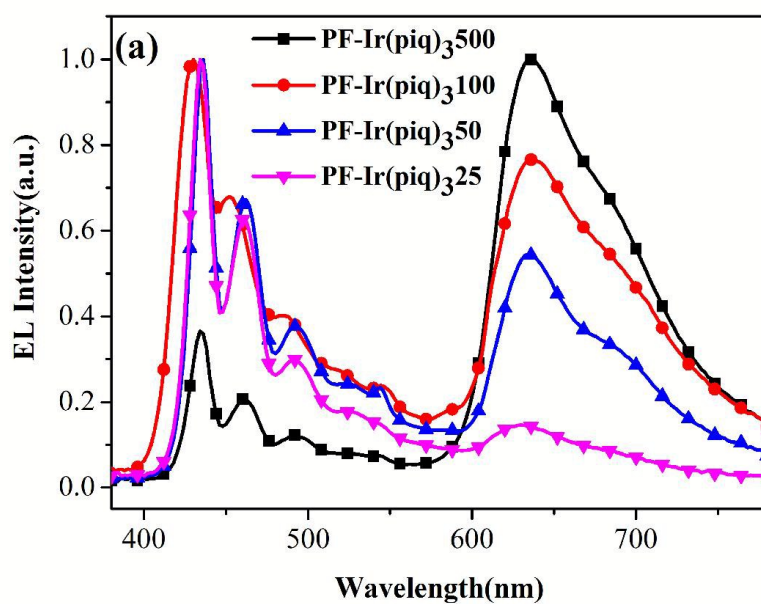
**Fig. 6** The energy transfer process of PF-Ir(piq)<sub>3</sub>m.

The energy transfer process is displayed in the Fig. 6. The three-dimensional structure has larger space steric hindrance and the delocalized  $\pi$ -electrons around PF backbones could be captured by iridium complex quickly. Due to the low content of Ir(piq)<sub>3</sub> below 0.5 mol%, the Förster energy transfer from the PF segments to the Ir(piq)<sub>3</sub> units is incomplete, which results in recombination emission of blue fluorescence of PF segments and red phosphorescence of Ir(piq)<sub>3</sub>.

### 3.5 Electroluminescent properties

The WPLEDs were fabricated with the configuration of ITO / PEDOT: PSS (40 nm) / PF-Ir(piq)<sub>3</sub>m (60 nm) / TPBI (40 nm) / LiF (1 nm) / Al (100 nm). As expressed in Fig. 7 (a), in EL spectra of PF-Ir(piq)<sub>3</sub>m, the red emission intensity enhance and blue emission intensity weaken with increasing of Ir(piq)<sub>3</sub> content in PF-Ir(piq)<sub>3</sub>m. The blue emission region has three emission band located at about 434 nm, 460 nm and 492nm, and the red emission at around 636 nm. The remarkable differences in PL and EL spectra imply that different mechanisms should be involved.<sup>47</sup> In PL process, the singlet excited states generate on the host chain of PF segments and subsequently transfer to the Ir(piq)<sub>3</sub> by Förster energy transfer. However, in EL process, direct charge trapping is dominated in the PF-Ir(piq)<sub>3</sub>m which induce stronger red emission intensity than those in PL plectra. At the same time, the energy transfer from PF segments to the red Ir(piq)<sub>3</sub> units is also effective.

Meanwhile, the PF branches directly connected with  $\text{Ir}(\text{piq})_3$  in hyperbranched framework that suppress the triplet–triplet (T–T) annihilation, the intramolecular energy transfer from the PF branch to  $\text{Ir}(\text{piq})_3$  would be also comparatively efficient. Furthermore, pure white-light emission could be realized by tuning the content of  $\text{Ir}(\text{piq})_3$  in  $\text{PF-Ir}(\text{piq})_3\text{m}$ . The Commission Internationale de l’Eclairage coordinates of all  $\text{PF-Ir}(\text{piq})_3\text{m}$  are expressed in Table 3. Among all hyperbranched polymers,  $\text{PF-Ir}(\text{piq})_3100$  shows the best Commission Internationale de l’Eclairage coordinates of (0.30, 0.23), which is close to pure white-light point (0.33, 0.33). The EL spectra of  $\text{PF-Ir}(\text{piq})_3100$  at different current density are also investigated as shown in the Fig. 7 (b). With the increasing current density, the red emission enhance slightly which indicate the hyperbranched  $\text{PF-Ir}(\text{piq})_3100$  has relatively good stability in the EL process.



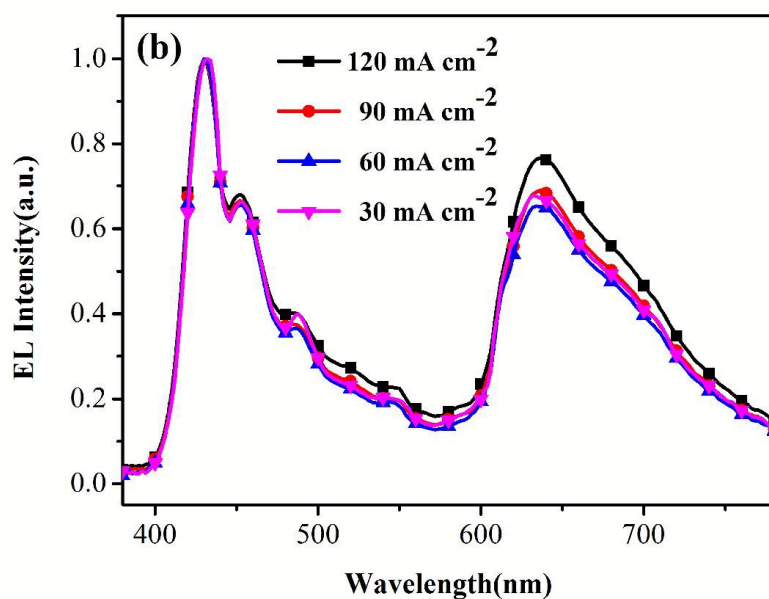


**Fig. 7** EL spectra of the PF-Ir(piq)<sub>3</sub>m (25, 50, 100 and 500) (a) and PF-Ir(piq)<sub>3</sub>100 at different current density (b).

**Table 3** Device performances of PF-Ir(piq)<sub>3</sub>m (25, 50, 100 and 500).

Polymers	$\lambda_{EL}/nm$	$L_{max}(cd/m^2)$	$LE_{max}(cd/A)$	CIE (x, y)
PF-Ir(piq) <sub>3</sub> 500	434/462/494/636	492	0.72	(0.46,0.27)
PF-Ir(piq) <sub>3</sub> 100	430/452/488/636	824	1.97	(0.30,0.23)
PF-Ir(piq) <sub>3</sub> 50	436/462/494/636	779	3.08	(0.28,0.23)
PF-Ir(piq) <sub>3</sub> 25	434/462/492/634	607	0.99	(0.22,0.19)

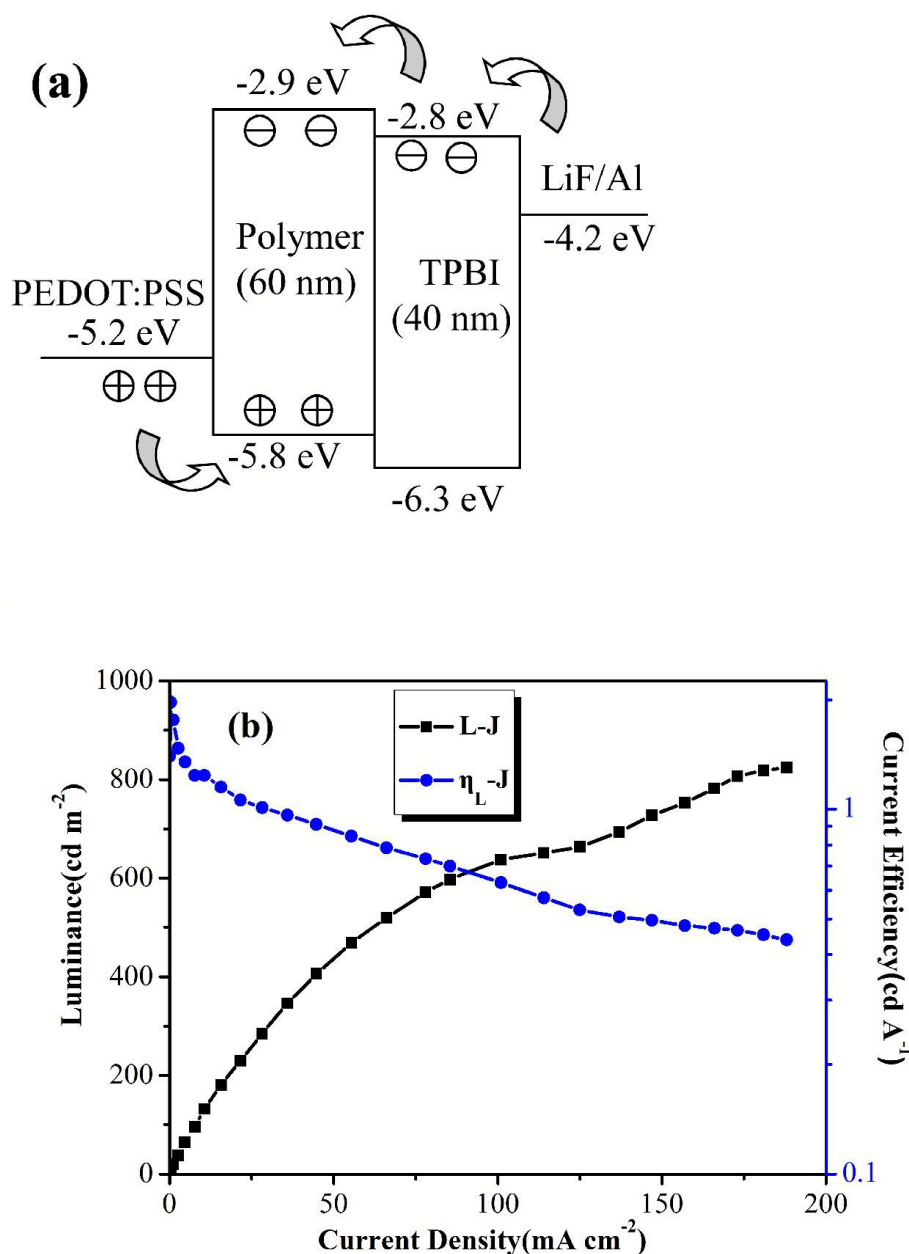


**Fig. 8** Schematic diagrams of the device configurations (a) and the Luminance-Current Density, Current Efficiency-Current Density curves (b).

Fig. 8 (a) shows the relative-energy-level diagram of the WPLED with the light-emitting layer of PF-Ir(piq)<sub>3</sub>100. The LUMO level of TPBI (-2.8 eV) matches better with the LiF/Al (-4.2 eV), at the same time the LUMO level of PF-Ir(piq)<sub>3</sub>100 (-2.90 eV) could match with the TPBI that makes the electrons injection and transmission easier. The HOMO level of the PF-Ir(piq)<sub>3</sub>100 is reduced 0.62 eV than PEDOT:PSS (-5.2 eV) with an injection barrier. By measurement, PF-Ir(piq)<sub>3</sub>100 reaches a maximum luminance of 825 cd m<sup>-2</sup> at 7.3 V and 9.15 mA cm<sup>-2</sup> with the LE 0.72 cd A<sup>-1</sup>.

Above results indicate that the incorporation of the Ir complexes into hyperbranched polymers with PF as branches is an effective way to fabricate the white light emitting devices. Further investigations on device optimization and the synthesis of polymers with different branches are ongoing in our laboratory.

#### 4. Conclusion

In summary, we have successfully demonstrated a series of hyperbranched polymers of PF-Ir(piq)<sub>3</sub>m with excited stable electrophosphorescent properties as the single emitting layer, by tuning different contents of Ir(piq)<sub>3</sub> covalently linked to the polyfluorene main chains efficiently. The PF-Ir(piq)<sub>3</sub>m have shown good solubility and thermal stability. Excellent energy transfer from the polyfluorene segments to Ir(piq)<sub>3</sub> units was identified by spectral analysis, and the three-dimensional structure could availablely suppress the Triplet-Triplet quenching. White light could be achieved by utilizing the hyperbranched structure with two components of polyfluorene and Ir(piq)<sub>3</sub> (0.1mol%) in a single-layer polymer. Among all hyperbranched polymers of PF-Ir(piq)<sub>3</sub>m, the PF-Ir(piq)<sub>3</sub>100 exhibits the best Commission Internationale de l'Eclairage coordinates of (0.30, 0.23), which is very close to pure white light.

**Acknowledgements:** This work was financially supported by Program for New Century Excellent Talents in University of Ministry of Education of China (NCET-13-0927); International Science & Technology Cooperation Program of China (2012DFR50460); National Natural Scientific Foundation of China (61205179, 61307030, 61307029); Shanxi Provincial Key Innovative Research Team in Science and Technology (2012041011).

#### References

- 1 R. H. Friend, R. W. Gymer, A. B. Holmes, J. H. Burroughes, R. N. Marks, C. Taliani, D. D. C. Bradley, D. A. Dos Santos, J. L. Bredas, M. Logdlund and W. R. Salaneck, *Nature* 1999, **397**, 121-128.
- 2 J. Liu, Q. G. Zhou, Y. X. Cheng, Y. H. Geng, L. X. Wang, D. G. Ma, X. B. Jing and F. S. Wang. *Adv. Funct. Mater.* 2006, **16**, 957-965.
- 3 C. Tang, X. D. Liu, F. Liu, X. L. Wang, H. Xu and W. Huang. *Macromol. Chem. Phys.* 2013, **214**,

314-342.

4 D. A. Poulsen, B. J. Kim, B. Ma, C. S. Zonte and J. M. J. Fréchet. *Adv. Mater.* 2010, **22**, 77-82.

5 T. H. Kim, H. K. Lee, O. O. Park, B. D. Chin, S. H. Lee and J. K. Kim. *Adv. Funct. Mater.* 2006, **16**, 611-617.

6 G. Cheng, T. Fei, Y. Zhao, Y. G. Ma and S. Y. Liu. *Org. Electron.* 2010, **11**, 498-502.

7 C. Fan, Y. H. Li, C. L. Yang, H. B. Wu, J. G. Qin and Y. Cao. *Chem. Mater.* 2012, **24**, 4581-4587.

8 M. Zhu, J. Zou, S. Hu, C. Li, C. Yang, H. Wu, J. Qin and Y. Cao, *J. Mater. Chem.*, 2012, **22**, 361-366.

9 H. Wu, G. Zhou, J. Zou, C.-L. Ho, W.-Y. Wong, W. Yang, J. Peng and Y. Cao, *Adv. Mater.*, 2009, **21**, 4181-4884.

10 J. Zou, H. Wu, C.-S. Lam, C. Wang, J. Zhu, C. Zhong, S. Hu, C.-L. Ho, G. Zhou, H. Wu, W. C. H. Choy, J. Peng and Y. Cao. W.-Y. Wong, *Adv. Mater.*, 2011, **23**, 2976-2980.

11 F. I. Wu, X. H. Yang, D. Neher, R. Dodda, Y. H. Tseng and C. F. Shu. *Adv. Funct. Mater.* 2007, **17**, 1085-1092.

12 C. H. Chien, S. F. Liao, C. H. Wu, C. F. Shu, S. Y. Chang, Y. Chi, P. T. Chou and C. H. Lai. *Adv. Funct. Mater.* 2008, **18**, 1430-1439.

13 H. J. Song, E. J. Lee, D. H. Kim, S. M. Lee, J. Y. Lee and D. K. Moon. *Synth. Met.* 2013, **181**, 98-103.

14 L. Ying, C. L. Ho, H. B. Wu, Y. Cao and W. Y. Wong. *Adv. Mater.* 2014, **26**, 2459-2473.

15 X. L. Yang, G. J. Zhou and W. Y. Wong. *J. Mater. Chem. C.* 2014, **2**, 1760-1778.

16 L. H. Liu, K. Q. Wu, J. Q. Ding, B. H. Zhang and Z. Y. Xie. *Polymer* 2013, **54**, 6236-6241.

17 Z. T. Liu, J. Liu, P. Cai and J. W. Chen. *J. Disp. Technol.* 2013, **9**, 490-496.

18 J. Liu, X. Guo, L. J. Bu, Z. Y. Xie, Y. X. Cheng, Y. H. Geng, L. X. Wang, X. B. Jing and F. S. Wang. *Adv. Funct. Mater.* 2007, **17**, 1917-1925.

- 19 S. Y. Shao, J. Q. Ding, T. L. Ye, Z. Y. Xie, L. X. Wang, X. B. Jing and F. S. Wang. *Adv. Mater.* 2011, **23**, 3570-3574.
- 20 L. Chen, P. C. Li, Y. X. Cheng, Z. Y. Xie, L. X. Wang, X. B. Jing and F. S. Wang. *Adv. Mater.* 2011, **23**, 2986-2990.
- 21 J. Liu, Y. X. Cheng, Z. Y. Xie, Y. H. Geng, L. X. Wang, X. B. Jing and F. S. Wang. *Adv. Mater.* 2008, **20**, 1357-1362.
- 22 L. Chen, P. C. Li, H. Tong, Z. Y. Xie, L. X. Wang, X. B. Jing and F. S. Wang. *J. Polym. Sci. Pol. Chem.* 2012, **50**, 2854-2862.
- 23 B. Du, L. Wang, H. B. Wu, W. Yang, Y. Zhang, R. S. Liu, M. L. Sun, J. B. Peng, Y. Cao. *Chem. Eur. J.* 2007, **13**, 7432-7442.
- 24 K. Zhang, Z. Chen, C. L. Yang, Y. T. Tao, Y. Zou, J. G. Qin and Y. Cao. *J. Mater. Chem.* 2008, **18**, 291-298.
- 25 L. Ying, Y. H. Xu, W. Yang, L. Wang, H. B. Wu and Y. Cao. *Org. Electron.* 2009, **10**, 42-47.
- 26 J. Zhang, S. Dong, K. Zhang, A. H. Liang, X. Y. Yang, F. Huang and Y. Cao. *Chem. Commun.*, 2014, **50**, 8227-8230.
- 27 Y. H. Li, H. Wu, C. S. Lam, Z. Chen, H. B. Wu, Wai-Yeung Wong and Y. Cao. *Org. Electron.* 2013, **14**, 1909-1915.
- 28 L. Ying, J. H. Zou, A. Q. Zhang, B. Chen, W. Yang and Y. Cao. *J. Organomet. Chem.* 2009, **694**, 2727-2734.
- 29 T. Guo, R. Guan, J. H. Zou, J. Liu, L. Ying, W. Yang, H. B. Wu and Y. Cao. *Polym. Chem.* 2011, **2**, 2193-2203.
- 30 L. Ying, L. Wang, A. Q. Zhang, Y. H. Xu, W. Yang and Y. Cao. *Chem. J. Chinese U.* 2010, **31**, 1480-1484.
- 31 R. Guan, Y. H. Xu, L. Ying, W. Yang, H. B. Wu, Q. L. Chen and Yong Cao. *J. Mater. Chem.* 2009, **19**, 531-537.

- 32 P. L. Burn, S. C. Lo and I. D. W. Samuel. *Adv. Mater.* 2007, **19**, 1675-1688.
- 33 M. J. Frampton, E. B. Namdas, S. C. Lo, P. L. Burn and I. D. W. Samuel. *J. Mater. Chem.* 2004, **14**, 2881-2888.
- 34 G. J. Zhou, W. Y. Wong, B. Yao, Z. Y. Xie and L. X. Wang. *Angew. Chem. Int. Ed.* 2007, **46**, 1149-1151.
- 35 J. C. Ostrowski, M. R. Robinson, A. J. Heeger and G. C. Bazan. *Chem. Commun.* 2002, 784-785.
- 36 A. Tsuboyama, H. Iwawaki, M. Furugori, T. Mukaide, J. Kamatani, S. Igawa, T. Moriyama, S. Miura, T. Takiguchi, S. Okada, M. Hoshino and K. Ueno. *J. Am. Chem. Soc.* 2003, **125**, 12971-12979.
- 37 H. Wang, Y. Xu, T. Tsuboi, H. X. Xu, Y. L. Wu, Z. X. Zhang, Y. Q. Miao, Y. Y. Hao, X. G. Liu, B. S. Xu and W. Huang. *Org. Electron.* 2013, **14**, 827-838.
- 38 Q. F. Yan, K. Yue, C. Yu and D. H. Zhao. *Macromolecules* 2010, **43**, 8479-8487.
- 39 N. R. Evans, L. S. Devi, C. S. K. Mak, S. E. Watkins, S. I. Pascu, A. Köhler, R. H. Friend, C. K. Williams and A. B. Holmes. *J. Am. Chem. Soc.* 2006, **128**, 6647-6656.
- 40 X. J. Zhang, M. A. Ballem, Z. J. Hu, P. Bergman and K. Uvdal. *Angew. Chem. Int. Ed.* 2011, **50**, 5729-5733.
- 41 H. Wang, J. L. Yang, J. Sun, Y. Xu, Y. L. Wu, Q. C. Dong, W. Y. Wong, Y. Y. Hao, X. W. Zhang and H. Li. *Macromol. Chem. Phys.* 2014, **215**, 1060-1067.
- 42 Y. Xu, H. Wang, C.L. Song, H.F. Zhou and B.S. Xu. *Chin. J. Lumin.* 2010, **31**, 274-278.
- 43 L. Ying, J. H. Zou, W. Yang, A. Q. Zhang, Z. L. Wu, W. Zhao and Y. Cao. *Dyes Pigments.* 2009, **82**, 251-257.
- 44 Q. L. Chen, N. L. Liu, L. Ying, W. Yang, H. B. Wu, W. Xu and Y. Cao. *Polymer* 2009, **50**, 1430-1437.
- 45 T. Guo, L. Yu, B. F. Zhao, Y. H. Li, Y. Tao, W. Yang, Q. Hou, H. B. Wu and Y. Cao. *Macromol. Chem. Phys.* 2012, **213**, 820-828.

46 J. L. Bredas, R. Silbey, D. S. Boudreaux and R. R. Chance, *J. Am. Chem. Soc.*, 1983, **105**, 6555-6559.

47 D. Hertel, S. Setayesh, H. G. Nothofer, U. Scherf, K. Müllen and H. Bässler. *Adv. Mater.* 2001, **13**, 65-70.